Surface Science 221 (1989) L750–L758
North-Holland, Amsterdam

SURFACE SCIENCE LETTERS

AN UNEXPECTED LOW-COVERAGE c(2 × 2) PHASE

N.C. BARTELT, L.D. ROELOFS * and T.L. EINSTEIN

Department of Physics, University of Maryland, College Park, MD 20742-4111, USA

Received 2 May 1989; accepted for publication 13 June 1989

We describe a lattice-gas model of adsorption on a square substrate in which an adsorbed p(2×2) phase disorders through an intermediate c(2×2) phase as the coverage is *lowered* from 1/4 of a monolayer. The occurrence of the low coverage c(2×2) phase can be understood in terms of a relatively small interfacial free energy between pairs of the four types of ordered domains in the p(2×2) phase. The diffraction features of this phase are indistinguishable from those of standard c(2×2) phases.

Overlayer phases of c(2 × 2) symmetry are often observed on square metallic surfaces [1]; they are often described in terms of lattice-gas models of adsorption [2]. Usually c(2 × 2) phases occur when nearly half of the available binding sites are occupied, as shown in fig. 1. In this paper we describe a lattice-gas system in which a c(2 × 2) phase occurs at much lower coverages – *less than 1/4 of a monolayer*. This phase is curious in that it lacks "local c(2 × 2) character": there are essentially no pairs of occupied second-neighbor sites. These aspects are so counter-intuitive that when we first encountered this phase in calculating the phase diagram of a lattice-gas model for Se/Ni(100) [3,4], we regarded it as spurious. The phase is, however, well defined and is an intermediate stage in the melting of a p(2 × 2) phase. In a diffraction experi-

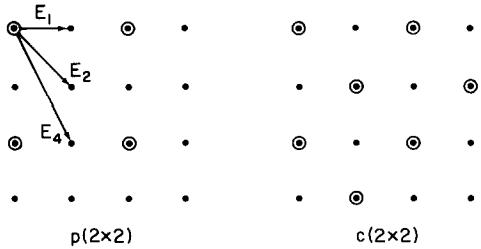

Fig. 1. Square lattice of binding sites depicting the standard structures and pairwise interaction energies discussed in the text.

* Permanent address: Department of Physics, Haverford College, Haverford, PA 19041, USA.

ment, this phase would display sharp beams at the positions characteristic of long-range c(2 × 2) order, with only diffuse intensity around those positions characteristic of p(2 × 2) order. This generic type of behavior is possible, of course, in the melting of any phase which can disorder through a sequence of phases of progressively higher symmetry [#1].

The interactions of the specific lattice-gas model we consider are shown in fig. 1. The interactions are chosen to yield a p(2 × 2) phase. The nearest neighbor interaction (E_1) is taken to be an exclusion and the second-nearest neighbor interaction (E_2) is assumed to be repulsive. The temperature–coverage phase diagram for the model with only E_1 and E_2 nonzero has been estimated by Kinzel and Schick [5]; it contains a c(2 × 2) phase near a coverage (θ) of 1/2 and a (2 × 1) phase around $\theta = 1/4$. To make the p(2 × 2) phase favorable compared to the (2 × 1) phase, either (1) $E_3 < 0$, assuming $E_4 = 0$, or more generally (2) $2E_4 > E_3$. Models with attractive E_3 interactions have coexistence regions at low temperatures and coverages [6] and thus do not readily exhibit the low-coverage c(2 × 2) phase. For convenience, we have taken $E_3 = 0$, and thus E_4 repulsive. As mentioned above, this model has been used to discuss Se/Ni(100): for the case $E_4 = 0.1E_2$, the phase diagram is given in refs. [3,4] for $k_B T > 3E_4$.

Fig. 2 shows the low-coverage phase diagram computed for the general case $E_2 \gg E_4$. The phase-boundary estimates were obtained by standard transfer-matrix scaling techniques [3–5] (for a review see refs. [7,8]); we compared strips of width 8 and 10. When $T \gg E_4/k_B$, the p(2 × 2) appears to disorder at a single temperature (or coverage): the distance between the two phase boundary estimates decreases with increasing strip width and does not depend sensitively on temperature [#2]. Once $T \lesssim E_4/k_B$, however, a c(2 × 2) phase appears between the p(2 × 2) and disordered phases. The existence of this phase can be best established at $T = 0$, where all the repulsions become exclusions; the consequent reduction in the number of allowed configurations makes it possible to work with larger strip widths, allowing more accurate estimates of the phase boundaries. Table 1 shows, for a sequence of pairs of increasing strip widths, the coverages at which long-range order appears at the (1/2, 1/2), (1/2, 0) and (0, 1/2) beams, as estimated by the scaling of the associated correlation length calculated using transfer matrices. Although the convergence with increasing strip width is not good enough to allow confident

[#1] We have observed similar behavior in the melting of a 2×1 phase in the square lattice-gas with equal first and second neighbor repulsions. In this case, the four-fold degenerate 2×1 phase sometimes melts via a phase with broken rotational symmetry (and no broken translational symmetry).

[#2] Another possibility is that the 2×2 phase disorders through a 2×1 phase rather than a c(2×2) phase. This might be expected to occur when the interaction which stabilizes the p(2×2) phase becomes much smaller than the temperature; it is observed to occur in models with small attractive E_3, for example.

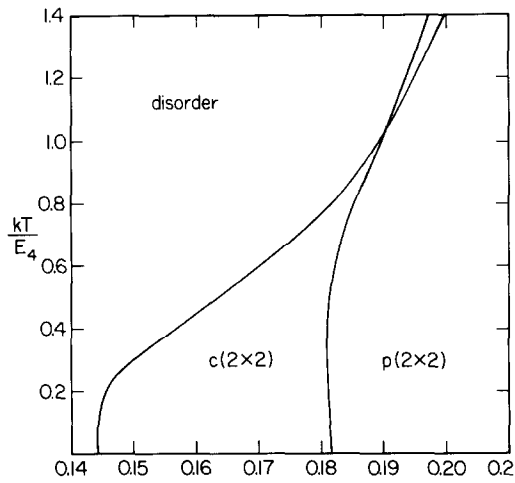

Fig. 2. Low-coverage portion of the phase diagram for the lattice-gas model defined in the text. The temperature is given in units of E_4: for $E_2 \gg E_4$ this phase diagram is independent of E_2. (For example, on the scale of the figure, the diagram for $E_4 = 0.1E_2$ is indistinguishable from the diagram for E_2 an exclusion.)

extrapolation to the infinite-system limit, it appears the onset of c(2 × 2) order is at $\theta \cong 0.15$, followed by p(2 × 2) order above $\theta \cong 0.18$. The finite-size scaling estimates for the critical exponent ν [7,8] are also given in table 1. Although the convergence is not good, the numbers seem consistent with a value of 1, characteristic of the Ising universality class. Ising behavior is consistent with the LGW classification of these two transitions [9] [#3].

The most interesting question about the low-coverage c(2 × 2) phase is its spatial character. If one started with a saturated c(2 × 2) phase and deleted 2/3 of its atoms to reach the coverage of this phase, the remaining "structure" could obviously not sustain order. To determine the nature of the low-coverage c(2 × 2) phase, we performed Monte Carlo simulations [#4]. Fig. 3 shows an illustrative sample configuration in the low-coverage c(2 × 2) phase. There is considerable local p(2 × 2) order, but no long-range p(2 × 2) order: Fig. 4

[#3] Much like the higher-coverage problem discussed in refs. [3,4], the phase diagram depicted in fig. 2 is expected to be topologically equivalent to the Ashkin–Teller model. Not only are the two boundaries of the low-θ c(2×2) region predicted to be Ising-like, but the p(2×2)–disorder boundary is expected to be in the class of the XY model with cubic anisotropy (as already predicted from the higher-coverage region [3,4]), while the point at which the lines join should be 4-state-Potts-like.

[#4] We performed 2×10^5 Monte Carlo steps per site in the grand canonical ensemble on a 96 × 96 lattice starting from an initially empty lattice. Fig. 3 is the final lattice configuration. Fig. 4 was obtained by averaging over every twentieth configuration of the final 150000 lattices.

Table 1
Critical-point estimates at zero temperature obtained with transfer-matrix scaling by comparing infinite strips of sites of width N and N'

	N, N'	θ_N^c,	z^c	ν
(1/2, 1/2)	6, 8	0.142434	2.315586	0.7887
	8, 10	0.144615	2.469382	0.8514
	10, 12	0.146208	2.570049	0.9008
	12, 14	0.146990	2.624710	0.9404
	14, 16	0.147226	2.650405	0.9728
	16, 18	0.147162	2.660012	0.9969
(1/2, 0)	6, 8	0.156653	2.873917	0.8405
	8, 10	0.163620	3.189939	0.8586
	10, 12	0.168234	3.376986	0.9617
	12, 14	0.171632	3.503852	0.9547
	14, 16	0.174245	3.596935	0.9962
	16, 18	0.176297	3.668678	1.0245
(0, 1/2)	6, 8	0.182807	4.173081	0.9755
	8, 10	0.181838	4.025126	0.9413
	10, 12	0.181352	3.946312	0.9617
	12, 14	0.181352	3.905662	0.9987
	14, 16	0.181304	3.886889	1.0361
	16, 18	0.181529	3.880351	1.0656

One first computes the appropriate correlation length $\xi_N^i = 2a/\ln(\lambda_0/|\lambda_i|)$, where λ_0 is the leading (real, non-degenerate) eigenvector of the transfer matrix for strip width N; the normalization by twice the lattice spacing (i.e. $2a$) arises because two rows at a time must be transferred (due to E_4). The estimate z^c, or more precisely $z^c(N, N')$, of the critical value of the activity ($z = e^{\mu/kT}$) is the solution of the scaling condition $N^{-1}\xi_N^i(z^c) = (N')^{-1}\xi_{N'}^i(z^c)$. In this problem there are three ξ's associated with long range order, corresponding to diffraction spots at (0, 1/2), (1/2, 0), and (1/2, 1/2), and so three independent criticality conditions. Using $z^c(N, N')$, one then computes the critical coverage $\theta_N^c = (z^c/N)\,d\lambda_0/dz|_{z^c}$ and obtains the correlation length exponent ν from $(N'/N)^{1+1/\nu} = (d\xi_{N'}^i/dz)/(d\xi_N^i/dz)|_{z^c}$. To determine λ_i one identifies the subblock of the transfer matrix which behaves appropriately under symmetry operations of the strip and finds the largest eigenvalues therein. In this case the important symmetry operation is cyclic permutation of the sites in a strip by one lattice constant. Taking the (0, 1) direction as the infinite direction of the strip, the eigenvector for (0, 1/2) is even under this operation; the associated λ is the second largest, λ_0 being the largest. The eigenvalues associated with (1/2, 0) and (1/2, 1/2) are the largest two in the subblock which is odd under the operation.

shows the result of a Monte Carlo computation of the structure factor [#5] in the low-coverage c(2 × 2) phase. There is clearly a delta function characteristic of c(2 × 2) long-range order at the (1/2, 1/2) position, but only diffuse intensity characteristic of short-range p(2 × 2) order around the (1/2, 0) position. As depicted in fig. 3, the reason there is long-range c(2 × 2) order is

[#5] For the particular definition of the structure factor used in fig. 4, see ref. [10].

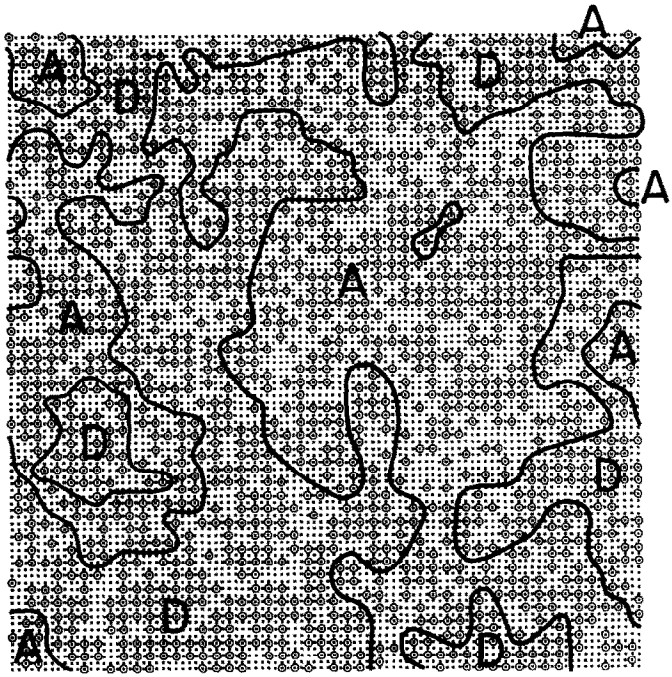

Fig. 3. Sample Monte Carlo configuration in the low coverage c(2×2) phase at $\theta \cong 0.162$ ($\mu = 0.23E_4$) and $k_BT = 0.2E_4$ on a 96×96 lattice. There is considerable short-range p(2×2) order, but two of the four possible p(2×2) domains (called A, B, C, and D in anticipation of fig. 5a) are preferentially occupied, leading to long-range c(2×2) order. In the figure, the occupations of sublattices A and D are comparable and well over an order of magnitude greater than the occupations of B or C.

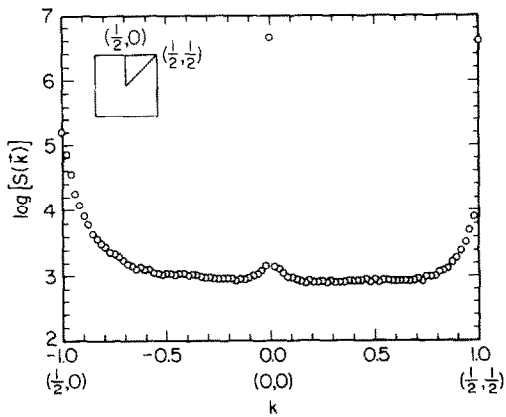

Fig. 4. Result of a Monte Carlo computation of the structure factor, $S(\boldsymbol{k})$, in the low-coverage c(2×2) phase at the same T and θ as in fig. 3.

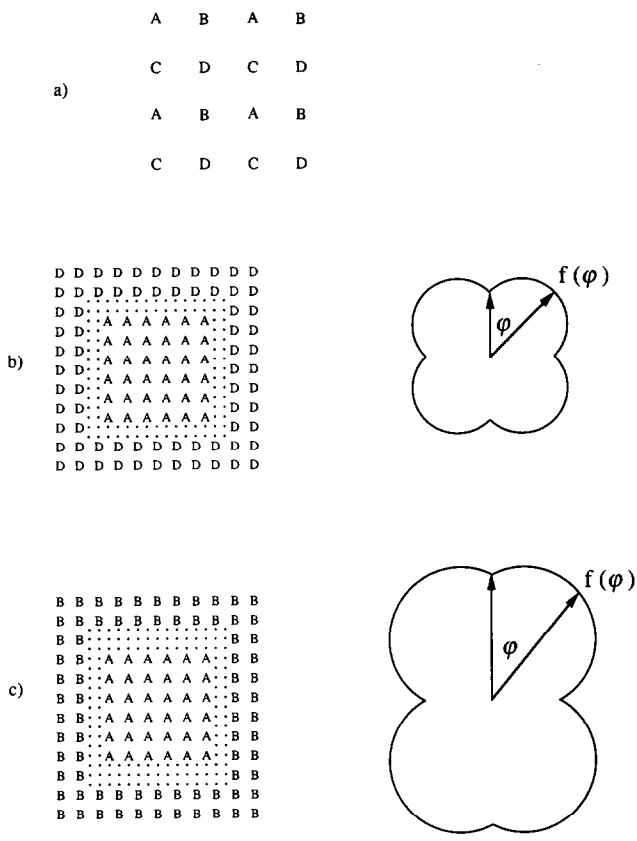

Fig. 5. Domain walls relevant to the structure of the low-coverage c(2×2) phase. Fig. 5a labels the four sublattices. Fig. 5b shows the A–D type of domains walls along with a polar plot of the orientational dependence of the interfacial tension $f(\varphi)$ in the limit of $T \to 0$ and $\theta \to 1/4$. Dots marking empty sites are included in the interface to help the reader visualize the "excess" free energy associated with the interface (see footnote #6); within a domain there would be one row of dots between each row of letters. Fig. 5c shows the the same picture as (b) but for A–B type interfaces. In this case $f(0) = 2f(90)$, and $f(90)$ is the same as in fig. 5b (see footnote #7).

that two of the four possible p(2 × 2) sublattices, lying on the same c(2 × 2) sublattice, are preferentially occupied.

From another viewpoint, the phase occurs due to the vanishing of the free energy of a particular type of domain wall in the p(2 × 2) phase. It is easy to see there are two distinct types of domain walls in a p(2 × 2) phase: Divide up the square lattice into four sublattices, A, B, C, and D, as shown in fig. 5a. Denote p(2 × 2) phases with predominant A, B, C, and D sublattice occupancy as A, B, C, and D phases, respectively. In the zero-temperature limit,

it is not hard to compute the interfacial (free) energy [#6]. Then, as seen in figs. 5b and 5c, A–D interfaces are rather different from A–B and A–C interfaces, the latter two possibilities being symmetrically equivalent. The difference can be seen, for example, in the dependence of the free energy on orientation, as shown to the right in figs. 5b and 5c [#7]. (The domain walls are drawn to avoid all E_4 bonds, as well as the even-more-repulsive E_1 and E_2 bonds.) The A–B and A–C walls are generally less dense than the A–D (or B–C) walls and so have a higher free energy near a coverage of 1/4. As one decreases the coverage below 1/4, the free energy of all walls decreases, with those of A–D character vanishing before those of A–B or A–C character. At and below the coverage at which the free energy of A–D walls vanishes, A–D walls will proliferate as shown in fig. 3, and the A and D (or B and C) sublattices will reach essentially equal occupancy of the A and D sublattices and very low occupancy of B and C (or the reverse). The resulting phase manifestly has long-range c(2 × 2) order. Remarkably, the phase exhibits no short-range c(2 × 2) order whatsoever – there are no E_2 bonds in fig. 3! (Thus, p(2 × 2) order will still be suggested by probes which are sensitive to order over a range less than a characteristic domain size; this size is related to the p(2 × 2) correlation length and so decreases as one moves away from the p(2 × 2) phase boundary.)

The existence of two types of domain walls in the p(2 × 2) phase allows interesting types of equilibrium behavior in p(2 × 2) melting. We next asked whether the novel behavior extends to kinetics: i.e. do the two types of domain walls also lead to interesting kinetics for the p(2 × 2) phase [#8]? For example, if the A–D domain walls were kinetically more difficult to remove in addition to being energetically favorable, they could lead to metastable low-coverage c(2 × 2) phases. We have in mind the rather common experimental situation of phase development at constant exposure. (This question occurred to us upon consideration of the unusual adsorption behavior seen in the system O/Pd(100) [13], where a metastable c(2 × 2) phase was observed which converted to a p(2 × 2) phase on annealing.) We accordingly developed a simulation to determine whether there are any anomalous kinetic effects intrinsic to the

[#6] At zero temperature all the repulsions become exclusions for $\theta < 1/4$; hence, as $\theta \to 1/4$, the free energy of an interface is proportional to the coverage deficit it causes. This is how the interfacial free energies in fig. 5 were obtained; that polar plots of the free energies consist of sections of circles is a general consequence of short-ranged pairwise interactions (cf. ref. [11]).

[#7] The interfacial free energies in the horizontal direction in figs. 5b and 5c are the same. This degeneracy will be broken by fluctuations (as the coverage is decreased), however. Because the interfacial free energies of the A–B interfaces shown in fig. 5c are everywhere else greater than those of the A–B interfaces of fig. 5b, it seems natural that fluctuations will also prefer the A–D interfaces in the horizontal direction.

[#8] The effect of different types of domain walls on kinetics has been studied, in a very similar situation, in ref. [12].

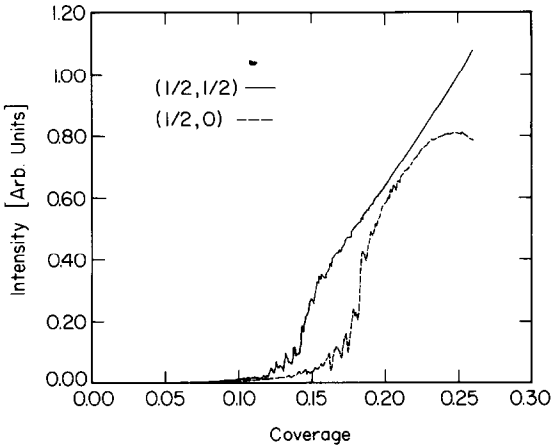

Fig. 6. Simulated time or coverage development of diffracted intensity at extra-beam positions for c(2×2) [i.e. (1/2, 1/2)] and p(2×2) phase [i.e. (1/2, 0)] during a constant adsorption-rate experiment, at $T = 0.2E_4/k_B$, on a 50×50 lattice. The curve for the (0, 1/2) beam is essentially indistinguishable from the (1/2, 0) beam on this scale.

low-coverage c(2 × 2) phase. (Our simulation is too crude to deal with the variety of extrinsic factors including defects, impurities, correlated motion, blocking effects in disassociation, etc., that might be experimentally significant [14].) Our code assumes (1) that the incident particles adsorb monatomically with sticking probability independent of either global or local coverage (except that no adsorption occurs into already occupied sites); (2) that once on the surface the adatoms can hop to first and second neighbor sites on the surface with the same attempt rate; and (3) that as the hopping proceeds, the overlayer tends toward local thermal equilibrium via standard equilibrium Monte Carlo dynamics based on the pairwise interaction energies (i.e. satisfying detailed balance). We chose a constant adsorption rate such that each adatom can attempt 600 hops in the time that the coverage increases by 0.001 monolayers.

The development of diffraction intensity at the high-symmetry positions as a function of coverage (or time) is shown in fig. 6. Under these conditions (1) the low-coverage c(2 × 2) phase does form in a well-ordered fashion at the appropriate coverage (as indicated by the parabolic increase of intensity with coverage); and (2) once formed, the phase does not appear to hinder subsequent development of the p(2 × 2) phase around a coverage of 0.18. Thus, if there is a system with interactions appropriate for producing this phase, there is no reason to assume it will be intrinsically hard to obtain for kinetic reasons. Secondly, without further limitations on the movement of adatoms, one sees an intermediate p(2 × 2) phase while progressing from the low-cover-

age c(2 × 2) to the saturation coverage c(2 × 2) (contrary to the observation described in ref. [13]).

The numerical work in this study was supported by the University of Maryland Computer Science Center and the National Center for Supercomputing Applications at the University of Illinois, at which the CRAY X-MP/48 was used. Computer time at the Pittsburgh Supercomputing Center was provided under NSF grant DMR-88-02986, which also provided partial support for N.C.B. and T.L.E. L.D.R. gratefully acknowledges support from the NSF under grant DMR-87-05568. L.D.R. and T.L.E. thank the Surface Science Division of Sandia National Laboratories, Livermore, CA, for hospitality during part of the preparation of the manuscript.

References

[1] H. Ohtani, C.-T. Kao, M.A. Van Hove and G.A. Somorjai, Progr. Surface Sci. 23 (1987) 155.
[2] L.D. Roelofs, in: Chemistry and Physics of Solid Surfaces IV, Ed. R. Vanselow (Springer, Berlin, 1982) p. 219.
[3] P. Bak, P. Kleban, W.N. Unertl, J. Ochab, G. Akinci, N.C. Bartelt and T.L. Einstein, Phys. Rev. Letters 54 (1985) 1539.
[4] N.C. Bartelt, PhD Thesis, University of Maryland, 1986, unpublished.
[5] W. Kinzel and M. Schick, Phys. Rev. B 24 (1981) 324.
[6] R.G. Caflisch and A.N. Berker, Phys. Rev. B 29 (1984) 1279.
[7] M.P. Nightingale, J. Appl. Phys. 53 (1982) 7927.
[8] J. Cardy, Ed., Finite-Size Scaling, Vols. 1 & 2 (North-Holland, Amsterdam, 1988).
[9] M. Schick, Progr. Surface Sci. 11 (1981) 245, and references therein.
[10] N.C. Bartelt, T.L. Einstein and L.D. Roelofs, Phys. Rev. B 35 (1987) 1776.
[11] C. Herring, Phys. Rev. 82 (1951) 87.
[12] A. Sadiq and K. Binder, J. Stat. Phys. 35 (1984) 517.
[13] S.-L. Chang and P.A. Thiel, Phys. Rev. Letters 59 (1987) 296.
[14] J.W. Evans, J. Chem. Phys. 87 (1987) 3038.